Characterization of the Denatured Structure of Pyrrolidone Carboxyl Peptidase from a Hyperthermophile under Nondenaturing Conditions: Role of the C-Terminal α-Helix of the Protein in Folding and Stability[†,‡]

Satoshi Iimura,[§] Taro Umezaki,[§] Makoto Takeuchi,[∥] Mineyuki Mizuguchi,[∥] Hiromasa Yagi,[⊥] Kyoko Ogasahara,[⊥] Hideo Akutsu,[⊥] Yasuo Noda,[§] Shin-ichi Segawa,[§] and Katsuhide Yutani*[,#]

School of Science and Technology, Kwansei Gakuin University, 2-1 Gakuen, Sanda, Hyogo 669-1337, Japan, Faculty of Pharmaceutical Sciences, University of Toyama, 2630 Sugitani, Toyama 930-0194, Japan, Institute for Protein Research, Osaka University, 3-2 Yamadaoka, Suita, Osaka 565-0871, Japan, and RIKEN SPring8-Center, Harima Institute, 1-1-1 Kouto, Sayo, Hyogo 679-5148, Japan

Received November 29, 2006; Revised Manuscript Received January 18, 2007

ABSTRACT: The cysteine-free pyrrolidone carboxyl peptidase (PCP-0SH) from a hyperthermophile, *Pyrococcus furiosus*, can be trapped in the denatured state under nondenaturing conditions, corresponding to the denatured structure that exists in equilibrium with the native state under physiological conditions. The denatured state is the initial state (D_1 state) in the refolding process but differs from the completely denatured state (D_2 state) in the concentrated denaturant. Also, it has been found that the D_1 state corresponds to the heat-denatured state. To elucidate the structural basis of the D_1 state, H/D exchange experiments with PCP-0SH were performed at pD 3.4 and 4 °C. The results indicated that amide protons in the C-terminal α6-helix region hardly exchanged in the D_1 state with deuterium even after 7 days, suggesting that the α6-helix (from Ser188 to Glu205) of PCP-0SH was stably formed in the D_1 state. In order to examine the role of the α6-helix in folding and stability, H/D exchange experiments with a mutant, A199P, at position 199 in the α6-helix region were performed. The α6-helix region of A199P in the D_1 state was partially unprotected, while some hydrophobic residues were protected against the H/D exchange, although these hydrophobic residues were unprotected in the wild-type protein. These results suggest that the structure of A199P in the D_1 state formed a temporary stable denatured structure with a non-native hydrophobic cluster and the unstructured α6-helix. Both the stability and the refolding rate decreased by the substitution of Pro for Ala199. We can conclude that the native-like helix (α6-helix) of PCP-0SH is already constructed in the D_1 state and is necessary for efficient refolding into the native structure and stabilization of PCP-0SH.

Small globular proteins are known to fold into the native state from the unfolded states in a simple two-state transition. However, in larger proteins, native structures are often formed via compact intermediate states (*1*−*7*). These compact intermediate states are rapidly formed and contain extensive secondary structures but lack the side chain packing which is formed in the native tertiary structure with a biological function. This intermediate state seems to correspond to the denatured states in equilibrium with the native state under physiological conditions. In order to understand the mechanism of the protein stability and protein folding, it is important to elucidate the structure of such a denatured state in equilibrium with the native state. Generally, these denatured states are transiently formed during the course of refolding from the fully extended denatured state in the concentrated denaturant, and their population in an equilibrium state is very low under physiological conditions. Therefore, it is very difficult to elucidate their structural details.

Fortunately, the refolding reaction of pyrrolidone carboxyl peptidase (PCP) from a hyperthermophile, *Pyrococcus furiosus*, is unusually slow at acidic pH and can be controlled by regulating the incubation temperature; it takes about 20 days to completely refold at pH 2.3 and 20 °C, and the refolding reaction significantly stops at pH 2.3 and 4 °C (*8*). The slow refolding kinetics is of great advantage in observing the denatured state transiently appearing during the refolding process. PCP is a homotetramer consisting of four subunits with 208 amino acid residues (molecular mass of 22.8 kDa). PCP contains two cysteine residues per subunit that do not form intramolecular disulfide bonds. Cysteine-free PCP (Cys144Ser/Cys188Ser; PCP-0SH)[1] is used for physicochemical experiments to avoid the formation of disulfide

[†] This work was supported in part by Grants-in-Aid 17570102 and 18031043 and the National Project for Protein Structural and Functional Analysis funded by the Ministry of Education, Culture, Sports, Science, and Technology of Japan.

[‡] The assigned chemical shifts for PCP-0SH and its mutant, A199P, have been deposited in the BMRB database with the accession number of 10052.

* To whom correspondence should be addressed. Phone: +81-791-58-2937. Fax: +81-791-58-2917. E-mail: yutani@spring8.or.jp.

[§] Kwansei Gakuin University.

[∥] University of Toyama.

[⊥] Osaka University.

[#] RIKEN SPring8-Center.

10.1021/bi602456y CCC: $37.00
Published on Web 02/20/2007

bonds. PCP-0SH exists as a tetramer in the region above pH 4.5, a dimer around pH 3.0, and a monomer below pH 2.7 (*9*). The refolding process of PCP-0SH from the fully denatured state in the concentrated denaturant has been studied by following the $^1H-^{15}N$ HSQC spectra in real time. During the refolding process of PCP-0SH, a stable intermediate (D_1 state) is immediately formed from the completely denatured state (D_2) in the concentrated denaturant and then refolds into the native state in a cooperative transition through an extremely slow reaction (*10*) as follows:

$$D_2 \leftrightarrow D_1 \leftrightarrow N$$

That is, the refolding of PCP-0SH from the D_1 state to the native state is highly cooperative without any intermediates between them, although the refolding rate is quite slow. This D_1 state corresponds to the denatured state in equilibrium with the native state under physiological conditions (*10*). In order to understand the cooperative transition from D_1 to N, it is important to elucidate the structural details of PCP-0SH in the D_1 state.

Hydrogen/deuterium (H/D) exchange experiments can provide information about the protein structure, structure change, dynamics, and folding (*11*). The H/D exchanges of amide hydrogens with deuterium atoms from deuterium oxide are catalyzed by hydroxide ions, water molecules, or hydroxonium ions depending on the pH condition (*12*). The reaction proceeds via formation of a transient complex between the amide hydrogen and these catalysts through hydrogen bonding. In order to elucidate the structural details of PCP-0SH in the D_1 state, the amide proton H/D exchange reactions of PCP-0SH were examined for individual residues. In general, the rates of the H/D exchange reaction of an amide proton are retarded by its hydrogen bonding to other proton acceptor atoms or by burying it in the interior of the protein (*13*). Therefore, the H/D exchange experiments with amide hydrogens provide information about the secondary structure formation of a specific residue. The NMR and CD studies of PCP-0SH in the D_1 state have suggested that the D_1 state is an ensemble of nonrandom structures with high helical contents, although the structural details are unknown (*10*). Therefore, an NMR study using a $^1H-^{15}N$ HSQC spectrum combined with H/D exchange experiments is a powerful method of observing the structure of PCP-0SH in the D_1 state at the level of individual amino acid residues.

In this paper, we first assigned the NMR signals of a $^1H-^{15}N$ HSQC spectrum in the native state of PCP-0SH. Furthermore, a Pro mutant, A199P, was prepared to examine the role of the C-terminal helix in the protein. Thereafter, in order to elucidate the structural details of PCP-0SH and A199P in the D_1 state, amide proton H/D exchange reactions were examined for the individual residues. The mechanism of folding and stability of PCP-0SH will be discussed on the basis of the structure of PCP-0SH in the D_1 state, that is, the denatured state in equilibrium with the native state under physiological conditions.

[1] Abbreviations: DSC, differential scanning calorimetry; H/D, hydrogen/deuterium; PCP-0SH, cysteine-free pyrrolidone carboxyl peptidase (Cys142/188Ser) from *Pyrococcus furiosus*; A199P, Pro mutant at position 199 of PCP-0SH (Ala199Pro); HSQC, heteronuclear single-quantum coherence; GuHCl, guanidine hydrochloride.

EXPERIMENTAL PROCEDURES

Protein Expression and Purification. PCP-0SH and its mutant Ala199Pro (A199P) from *P. furiosus* were expressed in the *Escherichia coli* strain JM109. The ^{15}N,^{13}C-double-labeled PCP-0SH was made by incorporating the ^{15}N-labeled NH_4Cl as the sole nitrogen source and the ^{13}C-labeled glucose as the sole carbon source in the M9 growth medium of 90% D_2O. Selective [^{15}N]Arg-, [^{15}N]Ile-, [^{15}N]Leu-, [^{15}N]Lys-, [^{15}N]Met-, [^{15}N]Tyr-, or [^{15}N]Val-labeled proteins were prepared by incorporating [^{15}N]Arg, [^{15}N]Ile, [^{15}N]Leu, [^{15}N]-Lys, [^{15}N]Met, [^{15}N]Tyr, or [^{15}N]Val, respectively, in a growth medium containing a mixture of the other unlabeled amino acids. Labeled and nonlabeled proteins were purified as already described (*10*, *14*). All of the purified proteins showed a single band on SDS−PAGE. The protein concentration was determined using the absorption coefficient of 0.66 at 278.5 nm in a quartz cell of 1 cm light path length for 1 mg/mL (*14*). Guanidine hydrochloride from Nakalai Tesque (Kyoto, Japan) was of specially prepared reagent grade and was used without further purification. Other chemical reagents were of special grade.

CD Measurements. The CD spectra were obtained using a Jasco J-600 spectropolarimeter. The far- and near-UV CD spectra were scanned nine times at a scan rate of 20 nm/min using a time constant of 2 s. The denaturation and refolding were also monitored by changes in the molar ellipticity at 222 and 280 nm after incubation for the desired time. The kinetic data were analyzed by the nonlinear least-squares method to determine the rate constant using the equation

$$Y(t) = Y_o + \sum A_i e^{-k_i t} \quad (1)$$

where $Y(t)$ is the signal value at the given time (t), Y_o is the signal value when no further change is observed, k_i is the apparent rate constant, and A_i is the total amplitude of the ith kinetic phase. A nonlinear least-squares calculation was carried out using Origin software (OriginLab).

NMR Experiments. All NMR measurements were carried out at a pH below 3.0, at which PCP-0SH exists in the monomeric or dimeric forms. The 3D HNCACB, HN(CO)-CACB, HNCO, HN(CA)CO, HSQC-NOESY-HSQC, and 2D $^1H-^{15}N$ HSQC spectra (*15*−*19*) for the NMR peak assignment were obtained using a Bruker DRX 800 spectrometer with ^{15}N,^{13}C-labeled PCP-0SH in a 20 mM Gly buffer of pH 2.5 at 30 °C. Selective [^{15}N]Arg-, [^{15}N]Ile-, [^{15}N]Leu-, [^{15}N]Lys-, [^{15}N]Met-, [^{15}N]Tyr-, or [^{15}N]Val-labeled proteins were also used to determine the kinds of amino acid residues of any peaks on a $^1H-^{15}N$ HSQC spectrum. Peak picking and editing were carried out using Sparky software (*20*). The assigned chemical shifts for PCP-0SH and its mutant, A199P, have been deposited in the BMRB database with the accession number of 10052.

The NMR spectra for the H/D exchange experiments were recorded using a Bruker Avance DRX 600 spectrometer equipped with a Bruker/SGI workstation. The apparent pH value, pH*, in the D_2O solution of the glass electrode was corrected by the relationship pD = pH* + 0.4 (*21*). The two-dimensional $^1H-^{15}N$ HSQC spectra with 256 × 1024 points in the t_1 and t_2 directions were collected.

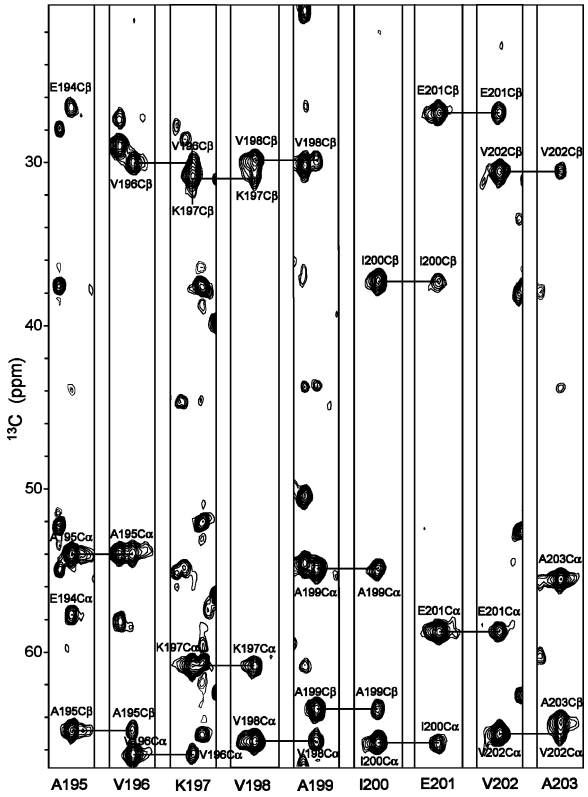

FIGURE 1: Sequential assignment of C-terminal α6-helix region of PCP-0SH at pH 2.5 and 30 °C. Sequential connectivity of $^{13}C^{\alpha}$ and $^{13}C^{\beta}$ between neighboring residues is shown as a strip plot derived from a 3D HNCACB spectrum.

RESULTS

NMR Peak Assignment of PCP-0SH. To examine the characteristic of PCP-0SH in the D_1 state, H/D exchange experiments were carried out with measurements of the $^1H-^{15}N$ HSQC spectra. In general, the $^1H-^{15}N$ HSQC spectra of proteins in the partially folded state, like a molten globule state, show a low spectral dispersion of broad cross-peaks and provide only little information. In fact, the $^1H-^{15}N$ HSQC spectra of PCP-0SH in the D_1 state have shown peak broadening (*10*). Consequently, the H/D exchange reaction could not be directly followed by the change in peak volume observed in the $^1H-^{15}N$ HSQC spectrum of PCP-0SH in the D_1 state. Therefore, after the H/D exchange reaction proceeded in the D_2O solution for PCP-0SH in the D_1 state, PCP-0SH was refolded into the native state, and the $^1H-^{15}N$ HSQC spectra were then obtained to detect the amide protons remaining undeuterated.

First, the peak assignment of the $^1H-^{15}N$ HSQC spectrum of PCP-0SH in the native state was necessary and performed as follows. The $^{15}N,^{13}C$-double-labeled PCP-0SH was prepared, and the standard arrays of amide $^1H-^{15}N$ edited through-bond connectivity experiments were obtained in order to attempt a sequential backbone assignment. The 3D HNCACB, HN(CO)CACB, HNCO, and HN(CA)CO experiments could successfully provide sequential connectivity between the amide $^1H-^{15}N$ and $^{13}C^{\alpha}$, $^{13}C^{\beta}$, carbonyl ^{13}C. Figure 1 shows a part of the sequential assignments as a strip plot for Ala195 to Ala203 involved in the C-terminal α6-helix. For the $^{13}C^{\alpha}$, $^{13}C^{\beta}$, and carbonyl ^{13}C resonances, 85% of the expected resonances was assigned. Figure 2 shows the $^1H-^{15}N$ HSQC spectrum of PCP-0SH in the native state at pH 2.5 and 30 °C. The chemical shift dispersion of this spectrum is typical of a folded protein. Due to the characteristics of the α-helical residues which show a low spectral dispersion in the spectrum, resonance peaks were concentrated in the central part of the spectrum. This made it difficult to perform the sequential assignment. Therefore, we used protein derivatives in which a specific amino acid was selectively labeled by ^{15}N. They were the [^{15}N]Arg-, [^{15}N]Ile-, [^{15}N]Leu-, [^{15}N]Lys-, [^{15}N]Met-, [^{15}N]Tyr-, and [^{15}N]Val-labeled proteins. Their $^1H-^{15}N$ HSQC spectra enabled us to assign many cross-peaks to a specific amino acid and to confirm the sequential assignment. As a result, the amide protons of 157 residues out of 192 theoretically assignable residues (16 Pro residues without an amide proton are included in 208 residues of PCP-0SH) could be assigned to specific amino acid residues. The assigned cross-peaks are labeled with the residue number on the $^1H-^{15}N$ HSQC spectrum (Figure 2).

H/D Exchange Experiments for PCP-0SH in the D_1 State. In order to characterize the structure of PCP-0SH in the D_1 state, which is the initial state in the refolding reaction, H/D exchange experiments were carried out under nondenaturing conditions. Using the experimental conditions at low temperatures (below 4 °C) at which the refolding reaction of PCP-0SH substantially stops (*8*), we performed H/D exchange experiments with PCP-0SH in the D_1 state. First, the PCP-0SH was completely denatured for 30 min in 6 M GuHCl at pH 2.0 and 60 °C. The PCP-0SH was then rapidly eluted into a D_2O solution at pD 3.4 and 4 °C through a PD-10 gel filtration column to remove the denaturant. By this treatment, PCP-0SH was transformed from the completely denatured state D_2 to the D_1 state, and the H/D exchange reaction in the D_1 state was initiated. After the H/D exchange reaction proceeded for the desired time, the temperature of the solution increased to 30 °C, at which the protein was completely refolded with a time constant of 6.0 min. After adjusting the pD to 2.9, the $^1H-^{15}N$ HSQC spectra of the deuterated PCP-0SH were obtained in the native state at 30 °C to detect the protected amide protons in the D_1 state.

Figure 3 shows the $^1H-^{15}N$ HSQC spectra of PCP-0SH, which was partially deuterated for various periods by the H/D exchange reaction in the D_1 state. The cross-peaks that disappeared from these spectra corresponded to amide protons involved in the region exposed to the solvent in the D_1 state, because such amide protons are exchanged with deuterium. As shown in Figure 3d, several peaks did not disappear even after the H/D exchange time of 24 h. The remaining amide protons are summarized in Figure 4. Strongly protected residues remaining after 12 h were Val145 and Leu193 to Glu205 involved in the C-terminal α6-helix region. Most residues in the C-terminal α6-helix composed of Ser188 to Glu205 were well protected against the H/D exchange reaction in the D_1 state. After 3 days, peaks in the $^1H-^{15}N$ HSQC spectrum completely disappeared except for those of the α6-helix. This means that only the α6-helix region stably forms a native-like structure in the D_1 state.

CD Spectra and Stability of A199P. In order to examine the role of the α6-helix formation in the D_1 state in the folding and stability, Ala at position 199 in the α6-helix region was substituted by Pro that would be expected to affect the α6-helix stability, because proline scanning experiments have suggested that the mutation at position 199 in

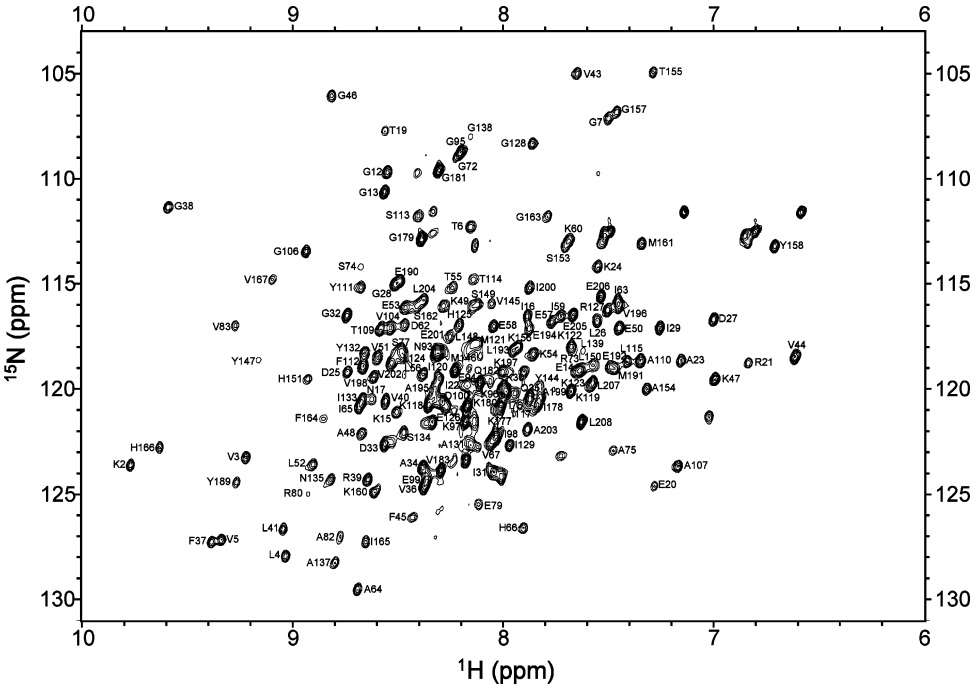

FIGURE 2: ^{1}H−^{15}N HSQC spectrum of PCP-0SH in the native state. The spectrum was obtained at pH 2.5 and 30 °C. Each label beside the resonance peaks on the spectrum shows the assigned amino acid residues.

the α6-helix region mostly affects the content of the α-helical structure of PCP-0SH in the D_1 state (Takeuchi and Mizuguchi, personal communication). In the native state at pH 2.4 and 25 °C, both PCP-0SH and A199P showed almost identical CD spectra in both the near- and far-UV regions (data not shown), suggesting that the native state structure is hardly affected by the mutation. To characterize the structure of the mutant of PCP-0SH, A199P, in the D_1 state, the far- and near-UV CD spectra were obtained at pH 2.4 and 4 °C (see Supporting Information, Figure S1). A199P in the D_1 state substantially decreased in ellipticity around 220 nm by the mutation, suggesting a decrease in the α-helical content compared to that of PCP-0SH.

To examine the stability of A199P, the pH dependence of the ellipticity at 280 nm was examined. CD measurements were carried out after various incubation periods in the pH region from pH 7.0 to 1.5 at 30 °C to examine when the acid-unfolding reactions reach equilibrium. In the acid pH region, although the ellipticity at 280 nm after 6 days was different from that after 30 days, the latter was identical to that after 60 days. Figure 5 shows the equilibrated acid denaturation curves of PCP-0SH and A199P after a 30-day incubation, indicating that A199P was less stable than the wild-type protein in the acidic pH region. The decrease in pH stability of A199P was also confirmed by differential scanning calorimetry (in preparation). Especially, the destabilization was remarkable below pH 2.5 where PCP-0SH exists in the monomer form.

To elucidate the role of α6-helix during folding, the refolding and unfolding kinetics of PCP-0SH and A199P were measured at pH 4 and 30 °C by monitoring the changes in the ellipticity at 222 nm (see Supporting Information, Figure S2). The unfolding reaction was initiated by manual mixing of the concentrated denaturant (GuHCl) into the solution of the native proteins. The refolding reaction was initiated by dilution of the GuHCl concentration after the proteins were completely denatured for 1 h in 6 M GuHCl at pH 4 and 60 °C. The refolding rate constants of PCP-0SH and A199P in the presence of 1.2 M GuHCl were 8.1 $\times$ 10^{-3} and 4.8 $\times$ 10^{-4} s^{-1}, respectively. The unfolding rate constants of PCP-0SH and A199P in the presence of 6.8 M GuHCl were 1.4 $\times$ 10^{-3} and 2.1 $\times$ 10^{-2} s^{-1}, respectively. The refolding and unfolding rates for the mutant A199P decreased and increased, respectively, by about 1 order relative to the wild-type protein PCP-0SH for the various GuHCl concentrations examined, indicating that A199P is less stable than PCP-0SH in an equilibrium state.

NMR Peak Assignment of A199P. Resonance peak assignments of A199P were carried out on the basis of the results for PCP-0SH. Because the chemical shifts of the many resonance peaks of A199P did not significantly change relative to those of PCP-0SH, many of the cross-peaks in the ^{1}H−^{15}N HSQC spectrum of A199P could be assigned only by comparison with those of PCP-0SH. However, several resonance peaks of A199P were significantly shifted from those of PCP-0SH. These peaks mostly originated from the regions close to position 199 in the tertiary structure. They were in the N-terminal half of the α1-helix, β4 and β5-strands, α3-helix, β8-strand, and β9-strand in addition to the α6-helix region itself as shown in Figure 6. This seems to arise from the distortion of the α6-helix region due to the substitution of Pro for Ala, because the α6-helix is in contact with these regions in the native structure. Assignment of these resonance peaks of A199P was performed using the 3D HSQC−NOESY−HSQC spectrum which provides the sequential connectivity between the neighboring amide nitrogens. In order to further confirm the sequential assignment, the [^{15}N]Ile-, [^{15}N]Leu-, [^{15}N]Lys-, [^{15}N]Met-, [^{15}N]Tyr-, or [^{15}N]Val-labeled A199P was also used as a protein sample effective for the peak assignment of a specific amino acid. The amide protons of 139 residues out of the theoretically assignable 191 residues could be assigned to specific amino acid residues in the ^{1}H−^{15}N HSQC spectrum of A199P at pH 3 and 25 °C (see Supporting Information, Figure S3).

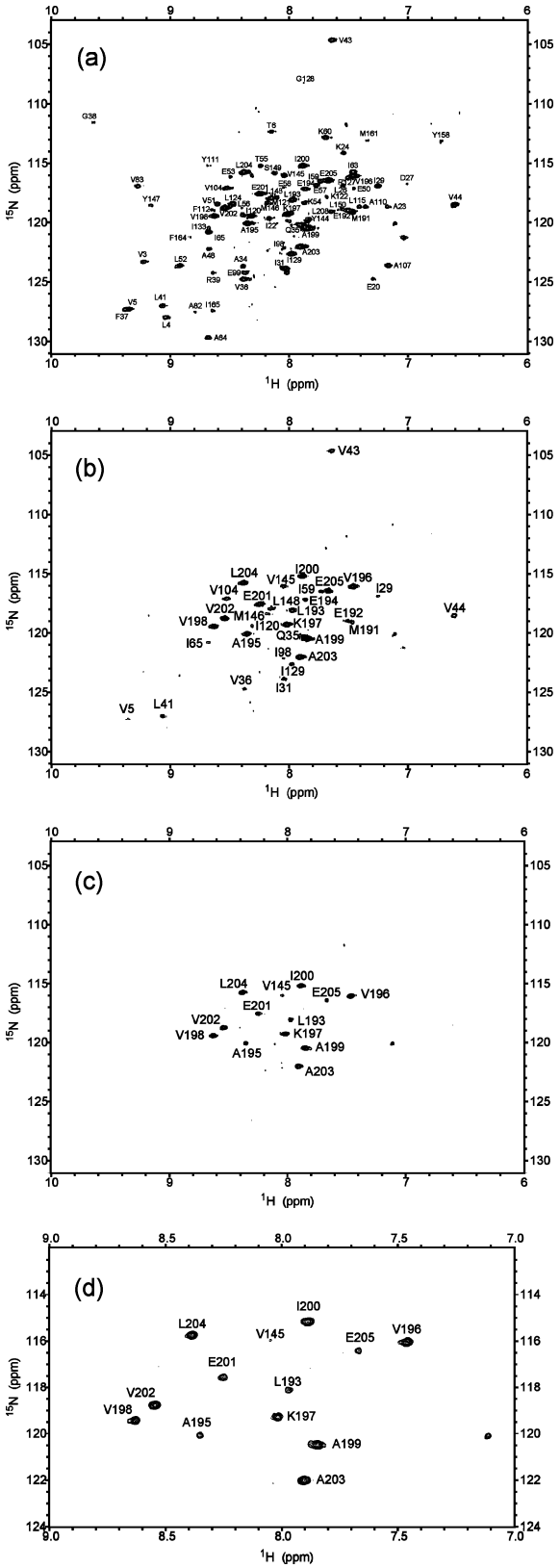

FIGURE 3: ^{1}H−^{15}N HSQC spectra of PCP-0SH refolded after the exposure to deuterium for 0 (a), 1 (b), 12 (c), and 24 h (d) in the D_1 state. These spectra were measured at pD 2.9 and 30 °C. Observable peaks indicate the undeuterated amide protons from residues of PCP-0SH in the D_1 state for each incubation time.

H/D Exchange Experiments for A199P in the D_1 State. To examine how the α6-helix region was affected in the D_1 state by the substitution of Pro for Ala199, the H/D exchange experiments for A199P in the D_1 state were carried out. Because an irreversible reaction occurred when A199P was incubated for over 60 min under the same conditions as for PCP-0SH (pD 3.4 and 4 °C), the H/D exchange reaction for

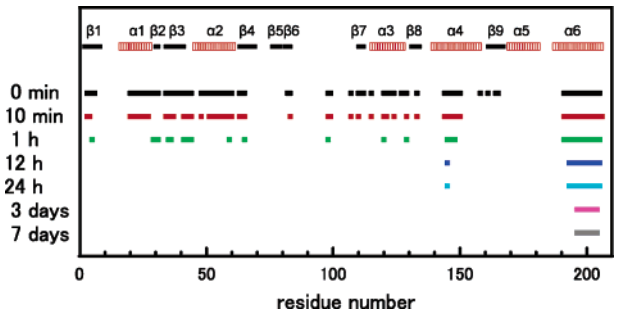

FIGURE 4: Summary of H/D exchange for amide protons on the amino acid sequence of PCP-0SH in the D_1 state at pD 3.4 and 4 °C. Each plot indicates residual amide protons after the H/D exchange reaction for each incubation time (0, 10 min, 1 h, 12 h, 24 h, 3 days, and 7 days). The secondary structure regions in the PCP-0SH tetramer determined by analysis of the X-ray crystal structure are also shown at the top of the figure.

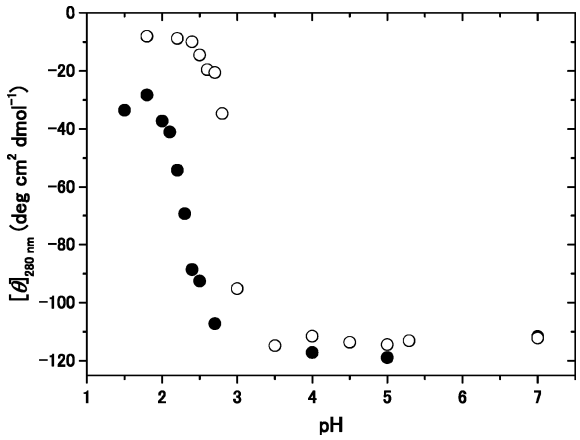

FIGURE 5: Structural stability of PCP-0SH and A199P versus pH. The acid denaturation of PCP-0SH (closed circle) and A199P (open circle) of native proteins was monitored by the ellipticity at 280 nm, $[\theta]_{280nm}$, to evaluate the stability of both proteins at 30 °C. $[\theta]_{280nm}$ reached equilibrium after 30 days at 30 °C. The CD value of PCP-0SH at pH 2.4 is about −90 in this figure at 30 °C and about −10 in the D_1 state (see figures in Supporting Information for details) at 4 °C. This means that the negative CD value in the D_1 state increases in value close to that of the native one when the temperature increases from 4 to 30 °C.

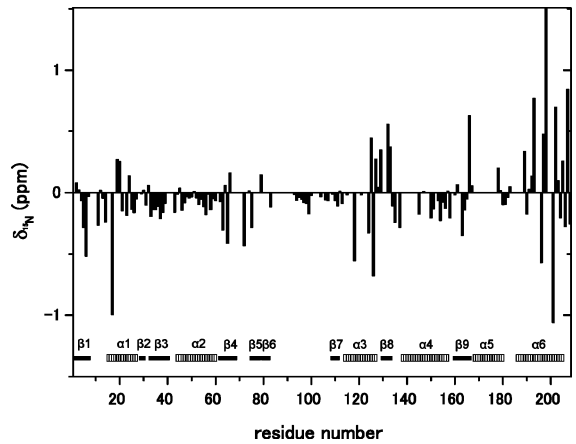

FIGURE 6: Chemical shift differences in the ^{15}N resonances of A199P from that of PCP-0SH at pH 3 and 25 °C are shown.

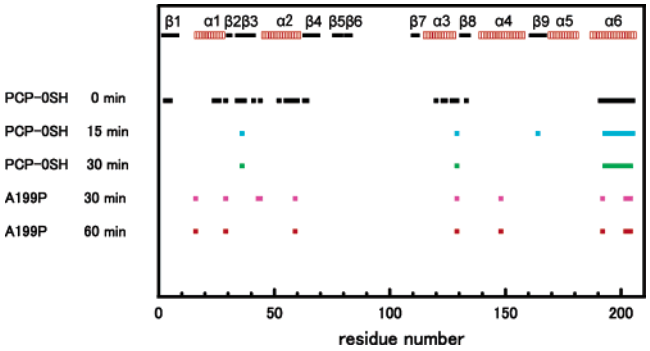

FIGURE 7: Summary of H/D exchange for amide protons in the amino acid sequence of PCP-0SH and A199P in the D_1 state at pD 4.5 and 4 °C is shown. Each plot indicates residual amide protons after the H/D exchange reaction for each incubation time.

A199P was performed at pD 4.5 and 4 °C. After this was accomplished for the desired time, A199P was rapidly refolded at 30 °C. The $^{1}H-^{15}N$ HSQC spectra for A199P in the native state were then measured at pD 3.0 and 25 °C (see Supporting Information, Figure S4). The amide protons of A199P remaining after the H/D exchange reaction for 30 min in the D_1 state were those in Ile16, Ile29, Leu41, Val43, Val44, Ile59, Ile129, Tyr147, Leu148, Glu192, and Val202 to Leu204 included in the C-terminal α6-helix region. Figure 7 shows the results of the H/D exchange experiments for A199P compared to those for PCP-0SH. In the case of A199P, the α6-helix region was partially unprotected in the D_1 state, indicating that the α6-helix became partially unstructured in the D_1 state due to the substitution of Pro for Ala. On the other hand, some hydrophobic residues (Ile16, Ile29, Leu41, Val43, Val44, Ile59, Ile129, Tyr147, and Leu148) still remained protected in the D_1 state after the H/D exchange for 30 min in spite of the fact that these residues in PCP-0SH completely disappeared after the H/D exchange for 15 min. They might form a hydrophobic cluster weakly associated in the D_1 state of A199P, although such a cluster was not found in the D_1 state of PCP-0SH. After a longer incubation at pD 4.5 and 4 °C, A199P began to leave the D_1 state for the native state. Therefore, it was difficult to determine the H/D exchange rates for these residues. Hydrophobic residues protected in the D_1 state of A199P are distributed over different secondary structural elements in the native state as shown in Figure 8. These residues might temporarily form a hydrophobic cluster different from the native conformation.

DISCUSSION

Structure of PCP-0SH in the Native State in Solution. The NMR peak assignment of PCP-0SH was performed under an acidic pH condition in which PCP-0SH exists in a monomeric form (*9*). The secondary structure of a protein can be speculated by the $^{13}C^{\alpha}$ resonance chemical shifts assigned to individual residues. In Figure 9, the chemical shift indices of PCP-0SH are plotted versus the residue number according to Wishart's rule (*22*). (I) If the chemical shift is greater than the range of the random coil chemical shift value for that residue, it is marked "1". (II) If the chemical shift is less than the range of the random coil chemical shift value for that residue, it is marked "−1". The local "density" of the nonzero chemical shift indices reflects the possibility of a secondary structure region, suggesting

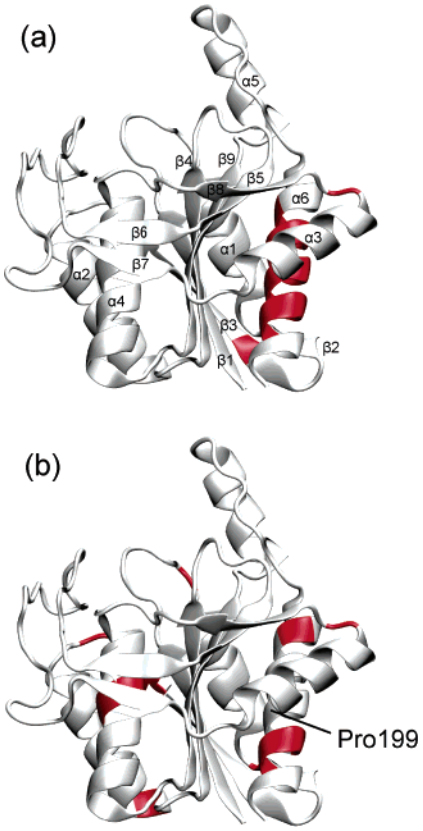

FIGURE 8: Ribbon diagrams of protected regions of PCP-0SH and A199P in the D_1 state. (a) and (b) represent protected regions in H/D exchange experiments in the D_1 state at pD 4.5 and 4 °C, shown in red on the tertiary structure for PCP-0SH and A199P, respectively. The figures were produced using VMD (*35*) and rendered with POV-Ray (www.povray.org) based on the X-ray crystallographic structure of PCP-0SH (PDB code 1IOI) (*23*).

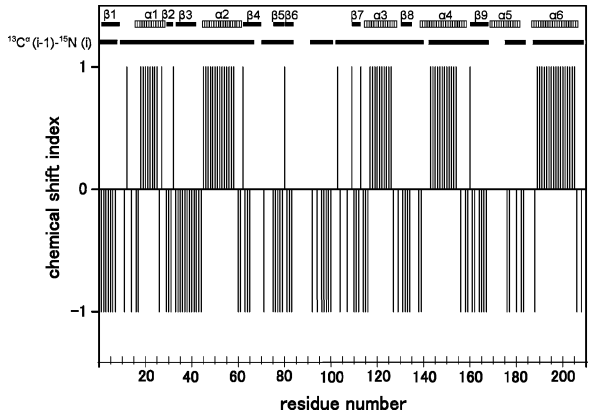

FIGURE 9: Chemical shift indices for the amino acid sequence of PCP-0SH using the $^{13}C^{\alpha}$ chemical shift values defined by the resonance peak assignments at pH 2.5 and 30 °C. The local densities of nonzero chemical shift indices reflect the possibility of a secondary structure formation in the regions. Sequential connectivity $^{13}C^{\alpha}(i-1)-^{15}N(i)$ obtained from the 3D HN(CO)CA spectrum is also shown in the filled squares above the chemical shift indices.

that a series of marks "−1" and "1" can assign the region to a β-strand and a helix, respectively. As shown in Figure 9, almost all of the secondary structure regions indicated by the chemical shift indices are consistent with those found in the X-ray crystalline structure in a tetrameric form (*23*) except for the α5-helical region. Although resonance peaks from the α5-helix region are assigned to only half of the residues, all of their chemical shift indices did not indicate

the possibility of an α-helix conformation. These results suggest that the α5-helix region might be at least partly unstructured in a monomeric form, although it seems to be stabilized due to an intersubunit hydrophobic interaction in a tetrameric form. The results of Figure 9 also confirm that the present peak assignment is reasonable.

D_1 State Structure of PCP-0SH. H/D exchange experiments of an amide proton provide information on its hydrogen bonding or its burial into a protein interior. The α-helix and *β*-sheet are stabilized by hydrogen bonding of an amide proton to a carbonyl oxygen, which retards the H/D exchange rate of the amide proton (*13*). PCP-0SH in the native state consists of six α-helices and nine *β*-strands. The H/D exchange experiments with PCP-0SH in the D_1 state showed that only the α6-helix region was strongly protected as shown in Figures 3 and 4. Protections against the H/D exchange reactions were evaluated from the intrinsic exchange time constant of each amino acid derived from a model peptide study (*24*). Some peaks, such as those of Gln35 and Val5, still remained in the $^1H-^{15}N$ HSQC spectrum after a 1 h exchange reaction in a D_2O solution and disappeared after 12 h (Figure 3b,c). They were not strongly protected from the solvent because their intrinsic time constants of the exchange changed from 81 (for Gln35) to 579 (for Val5) minutes under the conditions of pD 3.4 and 4 °C. One hour was not long enough for the amide protons of these residues to completely exchange. Although Va1145 was also protected for over 1440 min (24 h), it is only weakly protected from solvents because the intrinsic time of exchange is 409 min. On the other hand, residues in the central part of the α6-helix were strongly protected for over 10000 min (7 days). Their intrinsic time constants of exchange ranged from 111 (for Ala199) to 439 (for Ile200) min. Their protection factors are roughly estimated to be 23 (for Ile200) to 90 (for Ala199). H/D exchange studies for proteins in a molten globule state or kinetic intermediate states have indicated similar protection factor values (about 10−200) (*25*−*28*).

The substitution of Pro for Ala in the α6-helix region (A199P) affected the protection pattern against the H/D exchange reaction as shown in Figure 7. A hydrophobic cluster was found in the D_1 state of A199P. For residues involved in the hydrophobic cluster, it was difficult to estimate the time constants of the H/D exchange reaction, because the D_1 state did not persist long at pD 4.5 due to the initiation of refolding. The H/D exchange time of 60 min was not long enough compared to their intrinsic time constants of exchange ranging from 34 (for Ile59) to 136 (for Val43) min under the conditions of pD 4.5 and 4 °C. Under more acidic conditions, i.e., pD 3.4, A199P gradually changed from the D_1 state to an irreversible state where it could not be refolded into the native state, although the wild-type protein stably remained in the D_1 state for at least 7 days under the same conditions. This suggests that Ala199 plays an important role in avoiding the irreversible change in the D_1 state and in maintaining the initial state of refolding into the native state.

The propensity for secondary structure formation of proteins was predicted from their amino acid sequence (*29*). The amino acid sequence in the α6-helix region has a significantly high α-helix propensity relative to the other five helix regions as shown in Figure 10. It is likely that the helical structure remaining in the α6-helix region in the D_1 state is the origin for the intrinsic property of the short peptide that has a high α-helix propensity.

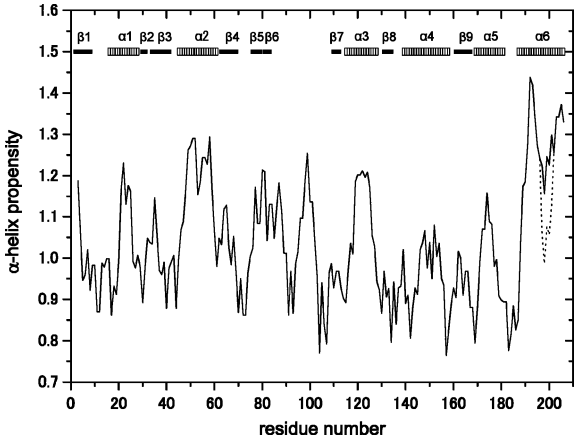

FIGURE 10: α-Helix propensity of PCP-0SH and A199P. The α-helix propensity of each residue was derived from the α-helix propensity value for each amino acid (*29*). The window size was set at 5 (residues), and an averaged value was calculated as the value for the middle residue in every five residues. The continuous and dotted lines indicate the α-helix propensity of PCP-0SH and A199P, respectively.

Effect of Proline Mutation on Stability and Refolding Kinetics. It is proposed that the stability of a protein can be increased by Pro substitution that decreases the conformational entropy of the unfolded state (*30*). H/D exchange experiments with PCP-0SH and A199P in the D_1 state indicated that the α6-helix is constructed in the D_1 state of PCP-0SH although it is partly destroyed in that of A199P. CD kinetic studies indicated a decrease in the refolding rate and an increase in the unfolding rate due to the mutation, suggesting that the stability of PCP-0SH is decreased by the Pro mutation at Ala199. This agrees with the acid denaturation results (Figure 5). This lower stability of A199P might be explained by the increase in entropy due to the difference in structures in the D_1 state, which is opposite the expectation.

For the slower refolding of A199P, the D_1 state is considered to be stabilized if the transition state was unchanged. However, the D_1 state of A199P appeared to be destabilized because it is not reasonable that A199P, which was regulated by its configuration of Pro199, is folded into the more stable denatured state than PCP-0SH with Ala199 under the same conditions. Therefore, the slower refolding and the faster unfolding of A199P seem to originate from the further destabilization of both the transition and native states by the Pro mutation relative to the destabilization of the D_1 state.

Implications for Structural Characterization in the Denatured State under Physiological Conditions. There are several reports of the structural characterization of a protein in the denatured state under nondenaturing conditions (*31*−*33*), although only in a few cases was the denatured protein sufficiently populated to permit direct structural characterization. The denatured states of the drkN SH3 domain in equilibrium with the native state under nondenaturing buffer conditions have been reported to have specific interactions leading to compact structures elucidated by the first strong NOE-based evidence (*32*). Under nondenaturing condition at neutral pH, the villin headpiece (HP67) has been observed

to exchange between the native state and a partially folded intermediate, in which the N-terminal domain is unfolded and the C-terminal domain is folded (*31*).

In the case of PCP-0SH in the D_1 state, a native-like α6-helix was found under nondenaturing conditions at acidic pH, but a non-native hydrophobic cluster was observed for A199P in the D_1 state. The non-native cluster of A199P might be only temporarily observed in the refolding process because A199P in the D_1 state could not remain in a stable state in the H/D exchange experiments. Therefore, the cluster of A199P in the D_1 state might be different from the actual denatured state in equilibrium with the native state under nondenaturing conditions unlike the structure of PCP-0SH in the D_1 state. The existence of the non-native structure during the refolding process has been found in equine *β*-lactoglobulin (*34*).

A single amino acid substitution remarkably affected the structure in the D_1 state, i.e., the denatured state in equilibrium with the native state under nondenaturing conditions. That is, by substitution of Ala with Pro at position 199, the formation of the non-native hydrophobic cluster and partial destruction of the α6-helix were observed in the D_1 state, and the D_1 state of A199P became unstable under some conditions, resulting in aggregation. These results reconfirm that it is important for understanding the mechanism of protein folding and stability to elucidate the structure in the denatured state under physiological conditions.

CONCLUSIONS

It is important to analyze the structural basis of the initial stage (intermediate state) of folding, corresponding to the denatured states in equilibrium with the native state under physiological conditions, in order to elucidate the mechanism of protein folding and stability. In this paper, the peak signals in the $^1H-^{15}N$ HSQC spectra of PCP-0SH and its mutant A199P were first assigned in their native states. Using the assigned signals and the H/D exchange reactions, we examined the structures of PCP-0SH and A199P in the D_1 state, corresponding to the denatured state in equilibrium with the native state under nondenaturing conditions at acidic pH. In the D_1 state of PCP-0SH, amide protons in the C-terminal α6-helical region hardly exchanged with deuterium even after a 7 day incubation during the H/D exchange experiments, indicating that the α6-helix of PCP-0SH is already constructed in the D_1 state. In the case of A199P, the α6-helix was partially destroyed when compared to PCP-0SH, in which hydrophobic residues temporarily form a non-native hydrophobic cluster with other hydrophobic residues. This partial destruction of the α6-helix and non-native residual structure in the D_1 state of the mutant protein also caused irreversible refolding after a long incubation time in the D_1 state at pD 3.4, although the refolding reaction of the wild-type protein was reversible even after a long incubation time in the D_1 state. It can be concluded that the C-terminal α-helix in the D_1 state plays an important role in retaining the D_1 state under the stable conditions and in correctly folding into the native structure of PCP-0SH.

ACKNOWLEDGMENT

We thank Takara Bio, Inc., for providing the PCP-0SH plasmid (pPCP3022).

SUPPORTING INFORMATION AVAILABLE

CD spectra of PCP-0SH and A199P in the D_1 state (Figure S1), typical refolding and unfolding curves of PCP-0SH and A199P (Figure S2), summary of NMR peak assignments of PCP-0SH and A199P (Figure S3), and $^1H-^{15}N$ HSQC spectra of A199P after the H/D exchange reaction (Figure S4). This material is available free of charge via the Internet at http://pubs.acs.org.

REFERENCES

1. Stigter, D., Alonso, D. O. V., and Dill, K. A. (1991) Protein stability: Electrostatics and compact denatured states, *Proc. Natl. Acad. Sci. U.S.A. 88*, 4176−4180.
2. Ogasahara, K., Matsushita, E., and Yutani, K. (1993) Further examination of the intermediate state in the denaturation of the tryptophan synthase α subunit: Evidence that the equilibrium denaturation intermediate is a molten globule, *J. Mol. Biol. 234*, 1197−1206.
3. Ogasahara, K., and Yutani, K. (1994) Unfolding-refolding kinetics of the tryptophan synthase α subunit by CD and fluorescence measurements, *J. Mol. Biol. 236*, 1227−1240.
4. Herrmann, L., Bowler, B. E., Dong, A., and Caughey, W. S. (1995) The effects of hydrophilic to hydrophobic surface mutations on the denatured state of iso-1-cytochrome *c*: Investigation of aliphatic residues, *Biochemistry 34*, 3040−3047.
5. Ogasahara, K., and Yutani, K. (1997) Equilibrium and kinetic analyses of unfolding and refolding for the conserved proline mutants of tryptophan synthase α subunit, *Biochemistry 36*, 932−940.
6. Poklar, N., Lah, J., Salobir, M., Macek, P., and Vesnaver, G. (1997) pH and temperature-induced molten globule-like denatuted states of equinatoxin II: A study by UV-melting, DSC, far- and near-UV CD spectroscopy, and ANS fluorescence, *Biochemistry 36*, 14345−14352.
7. Shimizu, S., and Chan, H. S. (2002) Origins of protein denatured state compactness and hydrophobic clustering in aqueous urea: Inferences from nonpolar potentials of mean force, *Proteins 49*, 560−566.
8. Kaushik, J. K., Ogasahara, K., and Yutani, K. (2002) The unusually slow relaxation kinetics of the folding-unfolding of pyrrolidone carboxyl peptidase from a hyperthermophile, *Pyrococcus furiosus*, *J. Mol. Biol. 316*, 991−1003.
9. Ogasahara, K., Khechinashvili, N. N., Nakamura, M., Yoshimoto, T., and Yutani, K. (2001) Thermal stability of pyrrolidone carboxyl peptidases from the hyperthermophilic Archaeon, *Pyrococcus furiosus*, *Eur. J. Biochem. 268*, 3233−3242.
10. Iimura, S., Yagi, H., Ogasahara, K., Akutsu, H., Noda, Y., Segawa, S., and Yutani, K. (2004) Unusually slow denaturation and refolding processes of pyrrolidone carboxyl peptidase from a hyperthermophile are highly cooperative: Real-time NMR studies, *Biochemistry 43*, 11906−11915.
11. Wand, A. J., and Englander, S. W. (1996) Protein complexes studied by NMR spectroscopy, *Curr. Opin. Biotechnol. 7*, 403−408.
12. Eigen, M. (1964) Proton transfer, acid-base catalysis, and enzymic hydrolysis, *Angew. Chem., Int. Ed. Engl. 3*, 1−19.
13. Milne, J. S., Mayne, L., Roder, H., Wand, A. J., and Englander, S. W. (1998) Determinants of protein hydrogen exchange studied in equine cytochrome c, *Protein Sci. 7*, 739−745.
14. Ogasahara, K., Nakamura, M., Nakura, S., Tsunasawa, S., Kato, I., Yoshimoto, T., and Yutani, K. (1998) The unusually slow unfolding rate causes the high stability of pyrrolidone carboxyl peptidase from a hyperthermophile, *Pyrococcus furiosus*: Equilibrium and kinetic studies of guanidine hydrochloride-induced unfolding and refolding, *Biochemistry 37*, 17537−17544.
15. Wittekind, M., and Mueller, L. (1993) HNCACB, a high-sensitivity 3D NMR experiment to correlate amide-proton and nitrogen resonances with the α- and *β*-carbon resonances in proteins, *J. Magn. Reson. B 101*, 201−205.
16. Grzesiek, S., and Bax, A. (1992) Improved 3D triple-resonance NMR techniques applied to a 31 kDa protein, *J. Magn. Reson. 96*, 432−440.
17. Clubb, R. T., Thanahal, V., and Wagner, G. (1992) A constant-time three-dimensional triple-resonance pulse scheme to correlate

intraresidue $^{1}H^{N}$, ^{15}N and $^{13}C'$ chemical shifts in $^{15}N-^{13}C$-labeled proteins, *J. Magn. Reson. 97*, 213−217.
18. Frenkiel, T., Bauer, C., Carr, M. D., Birdsall, B., and Feeney, J. (1999) HMQC−NOESY−HMQC, a three-dimensional NMR experiment which allows detection of nuclear overhauser effects between protons with overlapping signals, *J. Magn. Reson. 90*, 420−425.
19. Kay, L. E., Keifer, P., and Saarinen, T. (1992) Pure absorption gradient enhanced heteronuclear single quantum correlation spectroscopy with improved sensitivity, *J. Am. Chem. Soc. 114*, 10663−10665.
20. Goddard, T. D., and Kneller, D. G., SPARKY 3, University of California, San Francisco.
21. Glasoe, P. K., and Long, F. A. (1960) Use of glass electrodes to measure acidities in deuterium oxide, *J. Phys. Chem. 64*, 188−189.
22. Wishart, D. S., and Sykes, B. D. (1994) The ^{13}C chemical-shift index: A simple method for the identification of protein secondary structure using ^{13}C chemical-shift data, *J. Biomol. NMR 4*, 171−180.
23. Tanaka, H., Chinami, M., Mizushima, T., Ogasahara, K., Ota, M., Tsukihara, T., and Yutani, K. (2001) X-ray crystalline structures of pyrrolidone carboxyl peptidase from a hyperthermophile, *Pyrococcus furiosus*, and its Cys-free mutant, *J. Biochem. 130*, 107−118.
24. Bai, Y., Milne, J. S., Mayne, L., and Englander, S. W. (1993) Primary structure effects on peptide group hydrogen exchange, *Proteins 17*, 75−86.
25. Hughson, F. M., Wright, P. E., and Baldwin, R. L. (1990) Structural characterization of a partly folded apomyoglobin intermediate, *Science 249*, 1544−1548.
26. Lu, J., and Dahlquist, F. W. (1992) Detection and characterization of an early folding intermediate of T4 lysozyme using pulsed hydrogen exchange and two-dimensional NMR, *Biochemistry 31*, 4749−4756.
27. Jacobs, M. D., and Fox, R. O. (1994) Staphylococcal nuclease folding intermediate characterized by hydrogen exchange and NMR spectroscopy, *Proc. Natl. Acad. Sci. U.S.A. 91*, 449−453.
28. Guijarro, J. I., Jackson, M., Chaffotte, A. F., Delepierre, M., Mantsch, H. H., and Goldberg, M. E. (1995) Protein folding intermediates with rapidly exchangeable amide protons contain authentic hydrogen-bonded secondary structures, *Biochemistry 34*, 2998−3008.
29. Chou, P. Y., and Fasman, G. D. (1978) Prediction of the secondary structure of proteins from their amino acid sequence, *Adv. Enzymol. Relat. Areas Mol. Biol. 47*, 45−148.
30. Matthews, B. W., Nicholson, H., and Becktel, W. J. (1987) Enhanced protein thermostability from site-directed mutations that decrease the entropy of unfolding, *Proc. Natl. Acad. Sci. U.S.A. 84*, 6663−6667.
31. Grey, M. J., Tang, Y., Alexov, E., McKnight, C. J., Raleigh, D. P., and Palmer, A. G., III (2006) Characterizing a partially folded intermediate of the villin headpiece domain under non-denaturing conditions: Contribution of His41 to the pH-dependent stability of the N-terminal subdomain, *J. Mol. Biol. 355*, 1078−1094.
32. Mok, Y. -K., Kay, C. M., Kay, L. E., and Forman-Kay, J. (1999) NOE data demonstrating a compact unfolded state for an SH3 domain under non-denaturing conditions, *J. Mol. Biol. 289*, 619−638.
33. Zhang, O., and Forman-Kay, J. D. (1995) Structural characterization of folded and unfolded states of an SH3 domain in equilibrium in aqueous buffer, *Biochemistry 34*, 6784−6794.
34. Nakagawa, K., Tokushima, A., Fujiwara, K., and Ikeguchi, M. (2006) Proline scanning mutagenesis reveals non-native fold in the molten globule state of equine β-lactoblobulin, *Biochemistry 45*, 15468−15473.
35. Humphrey, W., Dalke, A., and Schulten, K. (1996) VMD−visual molecular dynamics, *J. Mol. Graphics 14*, 33−38.

BI602456Y